Cell, Volume *139*

Supplemental Data

An Epigenetic Switch Involving NF-κB, Lin28, Let-7 MicroRNA, and IL6 Links Inflammation to Cell Transformation

Dimitrios Iliopoulos, Heather A. Hirsch, and Kevin Struhl

SUPPLEMENTAL EXPERIMENTAL PROCEDURES

Chemicals and Reagents

Tamoxifen (TAM) that was used for induction of Src expression in MCF10A ER-Src cell was purchased by Sigma (H7904); Human recombinant IL6 that was used for cell treatments was purchased by Sigma (I1395) and the anti-IL6 monoclonal antibody (Mab206, R&D Systems); the antibody against Stat3 was purchased by Cell Signaling (cat no. 9139); the antibody against NF-κB (p65) was purchased by (Santa Cruz); the antibody against Lin28B was purchased by AbCam (ab71415); the antibody against Socs3 was purchased by AbCam (ab3693); the antibody against β-actin was purchased by Sigma (AC-15). Chemotherapy drug, doxorubicin, was purchased by Sigma (D1515). NF-kB pharmacological inhibitors, BAY-117082 was purchased by Calbiochem (cat no. 196870) and JSH-23 was purchased by Calbiochem (cat no.481408).

Phase-contrast Images

In order to study the morphological changes, phenotypic transformation and foci formation of MCF10A ER-Src TAM-induced (36h) cells, phase-contrast pictures were taken in a microscope (10x objective). Furthermore, phase-contrast pictures were taken MCF10A ER-Src cells induced by TAM for 36h and simultaneously treated with 100 nM of microRNAs (negative control, let-7d, let-7f, let-7a, let-7b, let-7c) or Ab-IL6 (2ug/ml) in order to study the effect of let-7 overexpression or IL6 inhibition in phenotypic transformation of MCF10A ER-Src cells.

Assessment of Transformation Efficiency by Src Activation

In order to study the efficiency and dynamics of Src activation we treated MCF10A ER-Src cells with 1uM tamoxifen for different time points (0, 5, 15, 30, 45, 60, 90, 120, 180, 240, 360 min), then washed 3 times with PBS and evaluated the percentage of transformation efficiency using phase-contrast images taken in the microscope (10x objective). In addition, we treated MCF10A ER-Src cells with 0.1 uM tamoxifen (10-fold dilution) and evaluated transformation efficiency. The experiments have been performed in triplicate.

Anoikis Assay

This assay was performed as described in Isakoff et al. (2005). Specifically, 6-well tissue culture plates were coated with 6 mg/mL poly-HEMA in 95% ethanol, incubated at 37^0C for several days until dry, and rinsed with PBS. MCF10A and MCF10A ER-Src (untreated and TAM-induced) cells were then plated at $4x10^5$/well in 2 ml growth medium for 36 h. Cells were collected and washed with PBS and apoptosis was measured using a Colorimetric Cell Death Detection ELISA kit according to the manufacturer's instructions (Roche Diagnostics,

Mannheim, Germany). Absorbance at 405 nm was measured and is reported with arbitrary units. Greater absorbance indicates greater apoptosis and histone release.

Cell Migration Assay

Untransformed and transformed MCF-10A ER-Src cells were starved overnight in assay medium (MCF10A growth medium containing 2% serum and no EGF). The starved cells were trypsinized, $1x10^5$ cells were added to the top chambers of the transwell (8 um pore size; BD Bioscience, Bedford, MA), and assay medium was added to the bottom chambers. For MCF7 cancer cells, the appropriate growth medium as recommended by ATCC was used instead of assay medium. After overnight incubation, the migratory cells were fixed and stained with 0.1% crystal violet solution. The experiment was repeated thrice and the statistical significance was calculated using Student's t test.

Invasion Assay

We performed invasion assays of untreated and 36h TAM-treated MCF10A ER-Src cells according to Gunawardane et al. (2005). Invasion of matrigel has conducted by using standardized conditions with BDBioCoat growth factor reduced MATRIGEL invasion chambers (PharMingen). Assays were conducted according to manufacturer's protocol, by using 5% horse serum (GIBCO) and 20 ng/ml EGF as chemoattractants.

Wound Healing Motility Assay

MCF10A, MCF10A ER-Src untransformed and transformed (36h TAM) cells were seeded onto six-well dishes at $1x10^5$/well. A single scratch wound was created using a p10 micropipette tip in to confluent cells. Cells were washed three times with PBS to remove cell debris, supplemented with assay medium, and monitored. Images were captured by phase-contrast microscopy using a 10x objective at 0, 12, and 24 h post wounding. To quantify the wounded area, we measured the area of the wound at the time of wounding (0 h) and at 12 (MCF10A ER-Src) or 24 hours (MCF10A, MCF10A ER-Src) post wounding to calculate the area of wound healing (Metamorph image analysis software). This area is represented as a percentage of the initial wound. The percentage of wound healing was averaged over three experiments and statistical significance was calculated using Student's t test.

MicroRNA Real-Time PCR Analysis

MicroRNA expression levels were tested using the mirVana qRT–PCR miRNA Detection Kit and qRT–PCR Primer Sets, according to the manufacturer's instructions (Ambion Inc, TX, USA). RNU48 expression was used as an internal control. The primers used for real-time PCR analysis of pri-let-7a3 were: forward: 5'-ACCAAGACCGACTGCCCTTT-3' and reverse: 5'-CTCTGTCCACCGCAGATATT-3' and for pri-let-7d were: forward: 5'-GCCAAGTAGAAGACCAGCAAG-3' and reverse: 5'-CAAGGAAACAGGTTATCGGTG-3'.

MicroRNA Target Prediction Analysis

The miRNA database miRBase (http://microrna.sanger.ac.uk/), the PicTar database (http://pictar.bio.nyu.edu/) and the TargetScan version 4.2 (http://www.targetscan.org/index.html) databases were used to identify potential miRNA targets. In order to have more accurate prediction results, we chose the targets genes that were predicted in two out of three databases and were conserved in other species.

Isolation of Let-7 Targets by miRNP Immunoprecipitation
HEK-293 cells were co-transfected with a plasmid that expressed HA-Ago1 together with 100 nM microRNAs (miR scramble as negative control or let-7a3), followed by HA-Ago1 immunoprecipitation (using HA-antibody). Real-time PCR analysis of the IP material was used to test the association of the IL6 mRNA with the RISC complex. Primers used for assessing IL6 mRNA expression were described below. Western blot analysis (for HA-tag) shows the efficiency of immunoprecipitation.

Real-time PCR analysis
Equal amounts of purified RNA samples from untreated and TAM-induced (1, 2, 4, 8, 12, 16, 24, 36h) MCF10A ER-Src cells were reverse-transcribed to form cDNA, which was subjected to SYBR Green based real-time PCR analysis. Primers used for β-actin forward: 5'-CCTGTACGCCAACACAGTGC-3' and reverse 5'- ATACTCCTGCTT GCTGATCC-3'; for IL1A forward: 5'-GCCAGCCAGAGAGGGAGTC-3' and reverse 5'-TGGAACTTTGGCCATCTTGAC-3'; for IL1B forward: 5'-GGCCCTAAA CAGATGAAGTGCT-3' and reverse 5'-TGCCGCCATC CAGAGG-3'; for IL6 forward: 5'-CCAGGAGCCCAGCTATGAAC-3' and reverse 5'-CCCAGGGAGAAGGC AACTG-3'; for IL8 forward: 5'-TTGGCAGCCTTCCTGATTTC-3' and reverse 5'-TCTTTAGCACTCCTTGGCAAAAC-3'; VEGF forward: 5'- GAG CCTTGCCTTGCT GCTCTAC-3' and reverse 5'- CACCAGGGTCTCGATTGGATG-3'; STAT3 forward: 5'-GCCAGAGAGCCAGGAGCA-3' and reverse 5'-ACACAGATAAACTTGGTCTTC AGGTATG-3'; JAK2 forward: 5'-TCGCTGTATCT GTCCACCTG-3' and reverse 5'-AGTCACTGGCACGGTTGTAG-3'; LIN28B forward: 5'-AGCCCCTTGGATATTCC AGTC-3' and reverse 5'- AATGTGAATTCCACTGGTTCTCCT-3'; . In addition, we have tested LIN28B mRNA expression levels in MCF10A ER-Src cells treated with tamoxifen and 5uM BAY-117082. The experiments have been performed in triplicate and data are presented as mean ± SD.

Interleukin 6 and VEGF ELISA Assays
The concentration of interleukin 6 and VEGF released to the supernatant of untreated and TAM-treated (1, 2, 4, 8, 12, 16, 24, 36h) MCF10A ER-Src cells was measured via IL6 ELISA assays (cat no. D6050) and VEGF ELISA assay (cat no. DVE00) according to manufacturer instructions (R&D Systems).

NF-kB/p65 ActivELISA Assay
The NF-kB/p65 ActivELISA Kit measured nuclear p65 levels in MCF10 ER-Src untreated or TAM-treated for 36h. The assay was performed in the same cells with the addition of siRNA-Ras (50nM) or the microRNA let-7a (50nM). In addition the assay was performed in MCF10-RAS^{V12} transformed cells and also MCF10A ER-Src sorted ($CD44^{high}/CD24^{low}$ and $CD44^{low}/CD24^{high}$) cells. The anti-p65 antibody coated plate captures free p65 and the amount of bound p65 is detected by adding a second anti-p65 antibody followed by alkaline phosphatase (AKP) -conjugated secondary antibody using colorimetric detection in an ELISA plate reader at absorbance 405nm. Each sample was loaded on triplicate and data are presented as mean ± SD.

Phospho-IκBα (Ser32) ELISA Assay
This assay (cat no 7276, Cell Signaling) is a solid phase sandwich enzyme-linked immunosorbent assay able to detect IκBα phosphorylation status (serine 32). The magnitude of the absorbance (450nm) is proportional to the quantity of bound target protein. We evaluated

IκBα phosphorylation status in untreated and 1uM TAM-treated (for 4h and 36h) MCF10A ER-Src cells, according to manufacturer instructions. Each sample was loaded on triplicate and data are presented as mean ± SD.

Multi-Spot Phospho-STAT3 (Tyr 705) Assay
This sandwich ELISA assay assessed the phosphorylation status of tyrosine 705 of STAT3 protein in untreated and TAM-treated (for 36h) MCF10A ER-Src cells. In some experiments these cells were also treated with increasing concentrations of let-7a (50, 80, 100 nM). Furthermore this assay was used to assess pStat3 in MCF10A ER-Src cells treated with IL6 (50ng/ml) or IL6 together with let-7a (50nM).

Western Blot Analysis
Cell lysates (30ug protein) from TAM-treated (for 36h) MCF10A ER-Src cells transfected also with 100 nM let-7a Ras protein levels were fractionated on 4%-20% SDS-polyacrylamide gradient gels (Bio-Rad) and transferred to Hybond-C membranes (Amersham Pharmacia). Membranes were blocked with 5% milk in PBS and then incubated with: anti-Ras (1:1,000 dilution, SC30, Santa Cruz); anti-Stat3 (1:1,000 dilution, 9139, Cell Signaling); anti-GAPDH (1:2,000 dilution, 2D4A7, Santa Cruz); anti-Lin28B (1:500 dilution, ab71415, AbCam) anti-β-actin (1:50,000 dilution, AC-15, Sigma). Detection was performed by using HRP-conjugated antisera (Amersham Pharmacia) and chemiluminescence.

Identification of NF-κB sites in let-7a3 and lin-28B
In order to identify NF-κB binding motifs in an area of 5kb upstream and 2kb downstream of both let-7a3 and lin-28B we used three selection criteria: 1) First we examined the presence of NF-κB binding motifs using Lever algorithm (Warner et al., 2008). Lever assesses whether the motifs are enriched in cis-regulatory modules (CRMs), in the noncoding sequences surrounding the genes; 2) For the identified binding sites we incorporated phylogenetic information from 12 different mammal species (mouse, rat, human, rabbit, chimp, macaque, cow, dog, armadillo, tenrec, opossum and elephant) and selected only the binding sites with high conservation scores (a conserved motif is considered one with a score higher than 200) by using PhylCRM algorithm (for more details see Warner et al., 2008). 3) Then, we mapped the conserved binding sites in the regions of interest, as well as visually inspecting the nucleosome occupancy in the conserved binding sites shown as part of the UCSC genome browser track. The top predicted and conserved NF-κB binding motif in let-7a was located in chromosome 22:44,883,275-44,883,284 and had a conservation score of 280.14, while the top predicted and conserved NF-κB binding motif in lin-28B was located in chromosome 6:105,511,974-105,511,983 and had a conservation score of 827.24.

Chromatin Immunoprecipitation
Chromatin immunoprecipitation was carried out as described previously (Yang et al., 2006). Briefly, the chromatin fragments, derived from untreated and TAM-treated (1, 4h) MCF10A ER-Src cells, were immunoprecipitated with 6ug of antibody against NF-κB(p65) (Santa Cruz). DNA extraction was performed using Qiagen Purification Kit. Real-time PCR analysis was performed for let-7a3 (forward: 5'- GGACAAGACCTTGCCGAAG-3' and reverse: 5'-CAGGACGAGGAAGGCTTG-3') (PCR product: 100bp) and lin-28B (forward: 5' TTACCCCAATACTGGG CATT-3' and reverse: 5'- GTGTGGGCGGTACAAAACAT-3') (PCR product: 103 bp).

LIN28B Luciferase assay

Luciferase assay: The putative NF-κB site (GGGGCTTTC) within the first intron of lin28b was either deleted or mutated to (TCATACGAT) by inverse PCR on the plasmid lin28b-P1 (Chang et al., 2009; this plasmid included an internal ribosome entry site (IRES) upstream of luciferase because several out-of-frame translation initiation codons were present in the cloned genomic fragment) using primer pairs TGCAAACCTATTGTTATAGATCTC and ACTGCGTGATGGGGGGTTGG or CGATTGCAAACCTATTGTTATAGATCTCC and TATGAACTGCGTGATGGGGG GTTGGG (mutated sequences are underlined), respectively. The PCR products were treated with T4 polynucleotide kinase (New England Biolabs) and self-ligated. The resultant plasmids lin28b-P1mut and lin28b-P1del were sequenced to confirm the deletion or the mutation of the putative NFkB site, respectively. These plasmids (lin28b-P1, lin28b-P1mut, lin28b-P1del) were transfected in MCF10A ER-Src TAM-treated cells and the luciferase activity was measured using the Dual Luciferase Reporter Assay System (Promega, WI, USA).

IL6 experiments

Luciferase assays: MCF10A cells transfected with pBabe-RAS^{V12} or pBabe-RAS^{V12} Ras and NF-κB inhibitor (BAY-117082) in 24-well plates were transfected using Lipofectamine. Firefly luciferase reporter gene construct (IL6-pGL3 vector was kindly provided by Dr William Farrar) (200 ng) and 1 ng of the pRL-SV40 Renilla luciferase construct (for normalization) were co-transfected per well. Furthermore, we performed luciferase assay using a luciferase reporter containing the 3'UTR of IL6 (IL6-luc) 24h after transfection with 100nM miR scramble or let-7a. Cell extracts were prepared 24h after transfection, and the luciferase activity was measured using the Dual Luciferase Reporter Assay System (Promega, WI, USA).

IL6-induced transformation: MCF10A cells were treated with 10-50ng/ml IL6 for 1h (short exposure). Induction of transformation was monitored by phase-contrast images and by using MetaMorph v5.0 program, the percentage of transformed cells was evaluated for 15 days. In addition, MCF10A cells treated with 50ng/ml IL6 for 1h were plated in soft agar and number of colonies were stained with crystal violet and counted 15 days later. Furthermore, IL6-treated MCF10A transformed cells for 15 days were treated with monoclonal antibody against IL6 (2ug/ml Ab-IL6) and with isotype antibody (2ug/ml Ab-IgG) as a control for 24h and cells were plated in soft agar. Number of colonies was counted 15 days later.

Oligonucleotide Transfection Experiments

MCF10A and derived cells were seeded in 6-well plates and were transfected with 100 nM siRNA against RAS (s806, Ambion Inc) or 50 nM siRNA against p65 (RelA) (s11914, Ambion Inc) or 80 nM siRNA against Stat3 (s744, Ambion Inc) or 80 nM siRNA against lin28b (s52477, Ambion Inc) or siRNA against Socs3 (s17190, Ambion Inc) or 50-100 nM of let-7a, let-7b, let-7c, let-7d, let-7f (Ambion Inc, TX, USA) using siPORT *NeoFX* transfection agent. SiPORT *NeoFX* is a lipid transfection agent consisting of a mixture of lipids that spontaneously complex small interference RNA and facilitates its transfer to the cells. Transfection with 50-100 nM siRNA control (AM4611, Ambion Inc) or miR-negative control (AM17110, Ambion Inc) were used as a control. No cell toxicity was detected due to the transfection agent. RNA was extracted in different time points after siRNA transfection and real-time PCR analysis was performed as described above. Beta-actin levels were used as loading control. All oligonucleotide transfection experiments were performed in triplicate.

FACS Analysis
Flow cytometric cell sorting was performed on single cell suspensions from untreated or TAM-treated for 1-360h MCF10A ER-Src cells and mammosphere-derived MCF10A ER-Src cells. Cells were stained with CD44 antibody (FITC-conjugated) (555478, BD Biosciences) and with CD24 antibody (PE-conjugated) (555428, BD Biosciences).

Xenograft experiments
Nude mice were maintained in accordance with Tufts Institutional Animal Care and Use Committee procedures and guidelines. $5x10^6$ MCF10A ER-Src untreated and TAM-treated (36h) cells were injected subcutaneously in the right flank of athymic nude mice (Charles River Laboratories). Tumor growth was monitored every five days and tumor volumes were calculated by the equation $V(mm^3)=axb^2/2$, where a is the largest diameter and b is the perpendicular diameter. When the tumors reached a size of ~100mm3 (15 days) were randomly distributed in 6 groups (5 mice/group). The first group was used as control (non-treated), the second group was i.p treated with 80nM siRNA negative control, the third group with 80nM siRNA against lin28b, the fourth group with a pharmacological inhibitor of NF-κB (5 uM BAY-117082), the fifth group with isotype antibody IgG (2ug/ml) and the sixth group with a monoclonal antibody against IL6 (2ug/ml). These treatments were repeated in a weekly basis for 3 cycles (days 15, 20, 25). In addition, $5x10^3$, $5x10^4$ and $5x10^5$ sorted $CD44^{high}/CD24^{low}$ and $CD44^{low}/CD24^{high}$ MCF10A ER-Src TAM-treated cells (36h), $5x10^6$ MCF10A ER-Src cells treated with 7uM JSI-124 or MCF10A cells treated with 50ng/ml IL6 or pBabe.Puro-lin28b were injected subcutaneously in athymic nude mice and tumor growth was monitored for 30 days.

Cancer Cell Line experiments
In this study we have used 15 different cancer cell lines (MCF7, SKBR3, MDA-MB-231, A549, H1299, Calu-6, A375, SK-MEL-28, HepG2, Panc-1, PC3, HeLa, Hep3B, Ovcar1, Caco2). In these cell lines lin28b, let-7 and IL6 expression levels were assessed by real-time PCR analysis.
In addition A549 (lung), HepG2 (hepatocellular), MDA-MB-231 (breast), PC3 (prostate) and Caco2 (colon) cancer cell lines were treated with 2 ug/ml Ab-IgG (control), 2ug/ml Ab-IL6, 80nM siRNA control, 80nM siRNA against LIN28B, 100nM microRNA scramble (control) and 100nM let-7 microRNA for 24h. The cells were plated in soft agar and colonies were counted 15 days later. The experiment has been performed in triplicate and data represent mean ± SD.
We assessed the motility and IL6 expression levels in A549, HepG2, MDA-MB-231, PC3 and Caco2 cancer cells after inhibition of IL6 (2ug/ml) expression by monoclonal antibody, inhibition of lin28b by siRNA (80nM) and overexpression of let-7 (100 nM) by cell migration assays and real-time PCR analysis respectively. Treatments with IgG antibody (2ug/ml), siRNA control (80nM) and scramble miR (100 nM) were used as experimental controls. The experiment was performed in triplicate and the mean ± SD is shown.

RNA Expression Studies from Patient Samples
RNAs from 22 ductal adenocarcinoma tissues and 10 normal mammary tissues; 21 prostate adenocarcinoma and 14 normal tissues; 15 hepatocellular carcinomas and 11 normal tissues and 15 lung adenocarcinomas and 5 normal tissues were purchased from Biochain (Hayward, CA) and Origene (Rockville, MD). In order to validate the absence of infiltrating macrophages which are frequently present in cancer tissues, we tested the expression of macrophage marker CD11b, which is not expressed in epithelial cells. In order to exclude the presence of immune RNA, in this study we have included only cancer tissues negative for CD11b expression (17/22 breast, 15/21 prostate, 9/15 hepatocellular, 11/15 lung cancer tissues). In these tissues we tested the

expression of lin28b, let-7a and IL6 by real-time PCR analysis. Each sample was run in triplicate and the data represent the mean ± SD. Correlation coefficient represents correlation between let-7 and IL6 expression levels in normal and cancer tissues.

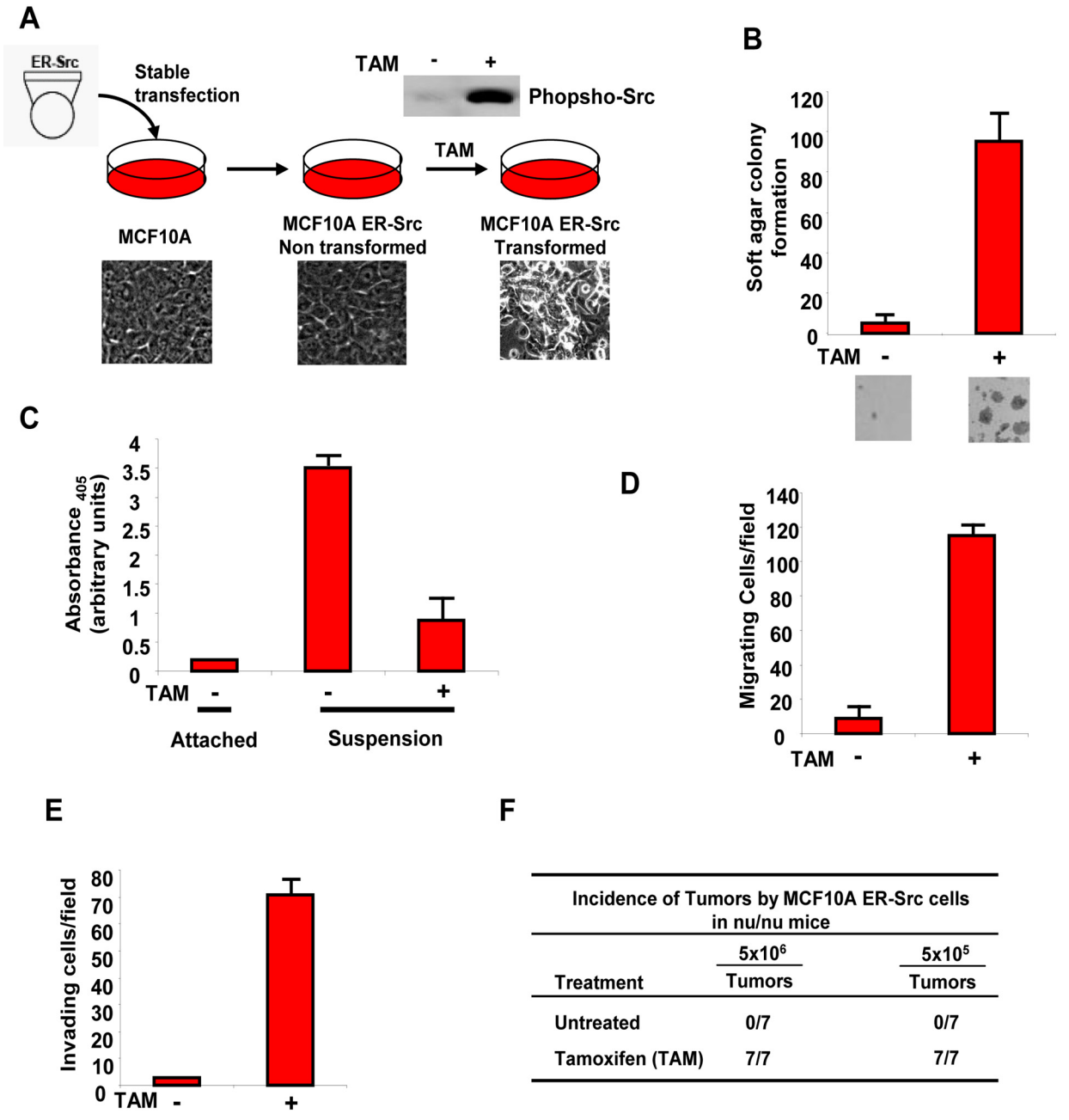

F

Incidence of Tumors by MCF10A ER-Src cells in nu/nu mice		
	$5x10^6$	$5x10^5$
Treatment	Tumors	Tumors
Untreated	0/7	0/7
Tamoxifen (TAM)	7/7	7/7

Figure S1. Isogenic Model of Epithelial Cellular Transformation. (A) Experimental steps and morphology (phase-contrast images) of MCF10A transformation model induced by Src kinase activation (western blot for phosphorylated Src Y419). **(B)** Soft agar colony assay of untransformed and transformed (+1uM TAM) MCF10A ER-Src cells **(C)** Anoikis anchorage-independent growth assay of attached and suspended MCF10A ER-Src cells and transformed (+TAM) MCF10A ER-Src cells. Results are plotted as arbitrary units of absorbance at 405 nm.

(D) Migration assay of and transformed (+TAM) MCF10A ER-Src cells. The experiment was performed in triplicate and the mean ± SD is shown. **(E)** Invasion assay of and transformed (+TAM) MCF10A ER-Src cells. The experiment was performed in triplicate and the mean ± SD is shown. (**F**) Untreated and TAM-treated MCF10A ER-Src cells were injected subcutaneously in the right flank of nu/nu mice. Tumor growth was monitored every 5 days for up to 1 month by observation and palpation.

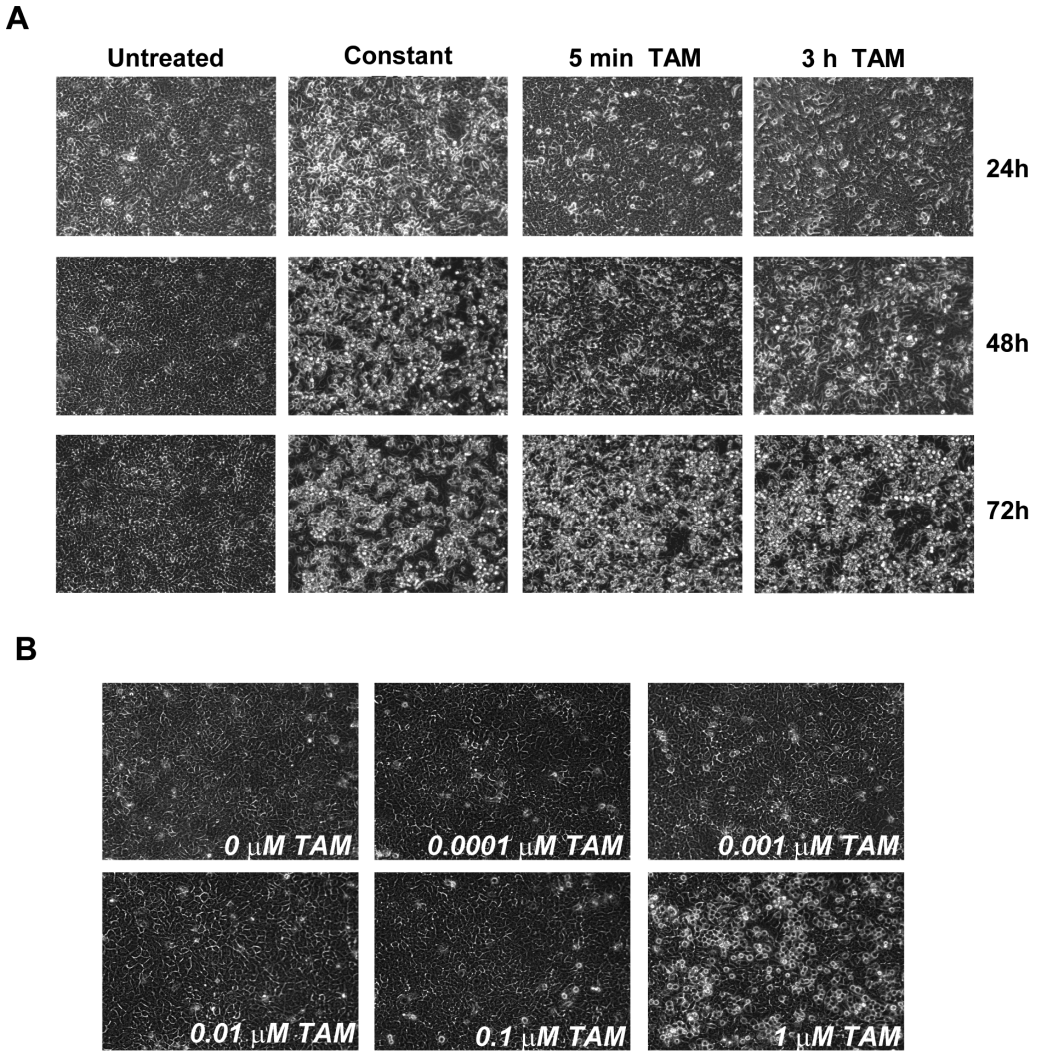

Figure S2. Dynamics of MCF10A ER-Src transformation. (A) Delayed Transformation of 5 min and 3h TAM-induced MCF10A ER-Src cells. Phase contrast images were taken from untreated and 1uM TAM-treated MCF10A ER-Src cells. Constant TAM treatment resulted in transformation of MCF10A ER-Src cells 24h post TAM treatment. On the other hand treatment with TAM for 5min or 3h and then withdrawal from the culture media resulted in delayed transformation, detected 48-72h post TAM treatment. **(B) Phase contrast images of MCF10A ER-Src cells treated with different doses of tamoxifen (144h post treatment).** MCF10A ER-Src cells were treated with serial dilutions of Tamoxifen and photographs were taken 144 hours post treatment. There is little transformation (<5%) in any concentration other than 1 uM tamoxifen.

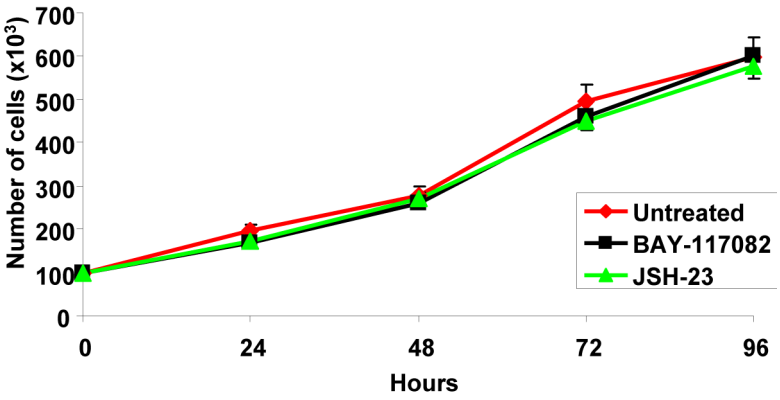

Figure S3. Inhibition of NF-κB pathway does not affect growth of untransformed MCF10A ER-Src cells. MCF10A ER-Src cells were treated with 5uM of BAY-117082 (inhibitor of IκBα phosphorylation) and 6uM of JSH-23 (selective blocker of the nuclear translocation of NF-κB p65) and cell growth was assessed every day for 4 days. The experiment was performed in triplicate and data represent mean ± SD.

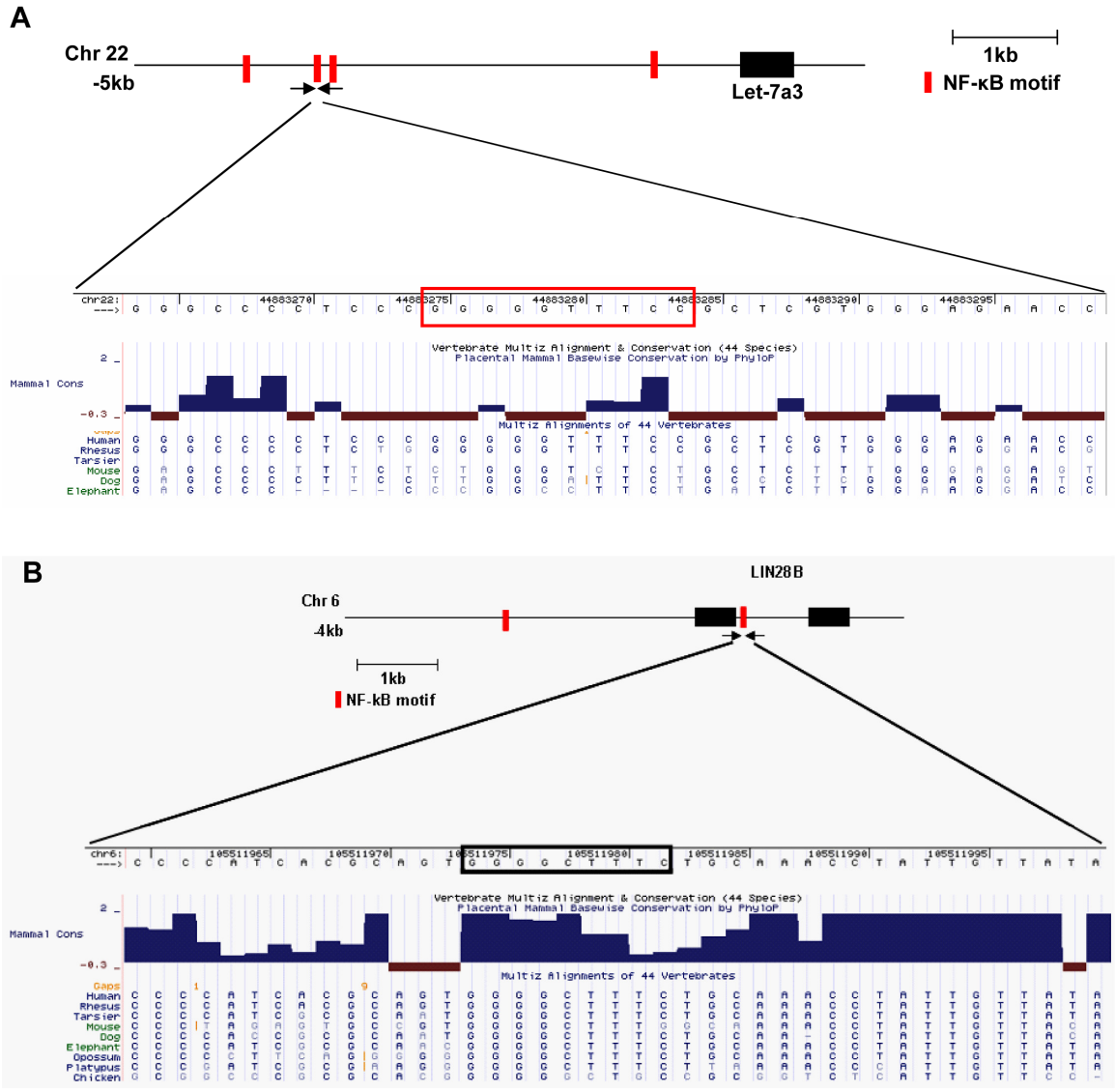

Figure S4. Identification of NF-κB binding motifs in let-7a3 and lin28b (A) Bioinformatic analysis (described in supplementary methods) revealed 4 potential NF-κB binding sites upstream of let-7a3 and let-7b. According to this analysis the most conserved NF-κB site was located around 4kb upstream from let-7a3 (chr22: 44,883,250-44,883,300). In the red box is shown the NF-κB binding motif in this site (GGGGGTTTCC) and its conservation in different species. We have designed primers around this site and performed chromatin immunoprecipitation. **(B)** Bioinformatic analysis revealed two potential NF-κB binding sites one upstream and one downstream of lin-28B TSS. Using this program we identified very high sequence conservation of the NF-KB binding motif located downstream (intron 1) of lin-28B TSS. In the black box is shown the NF-κB binding motif in this site (GGGGCTTTC) and its conservation in different species. We have designed primers around this site and performed chromatin immunoprecipitation.

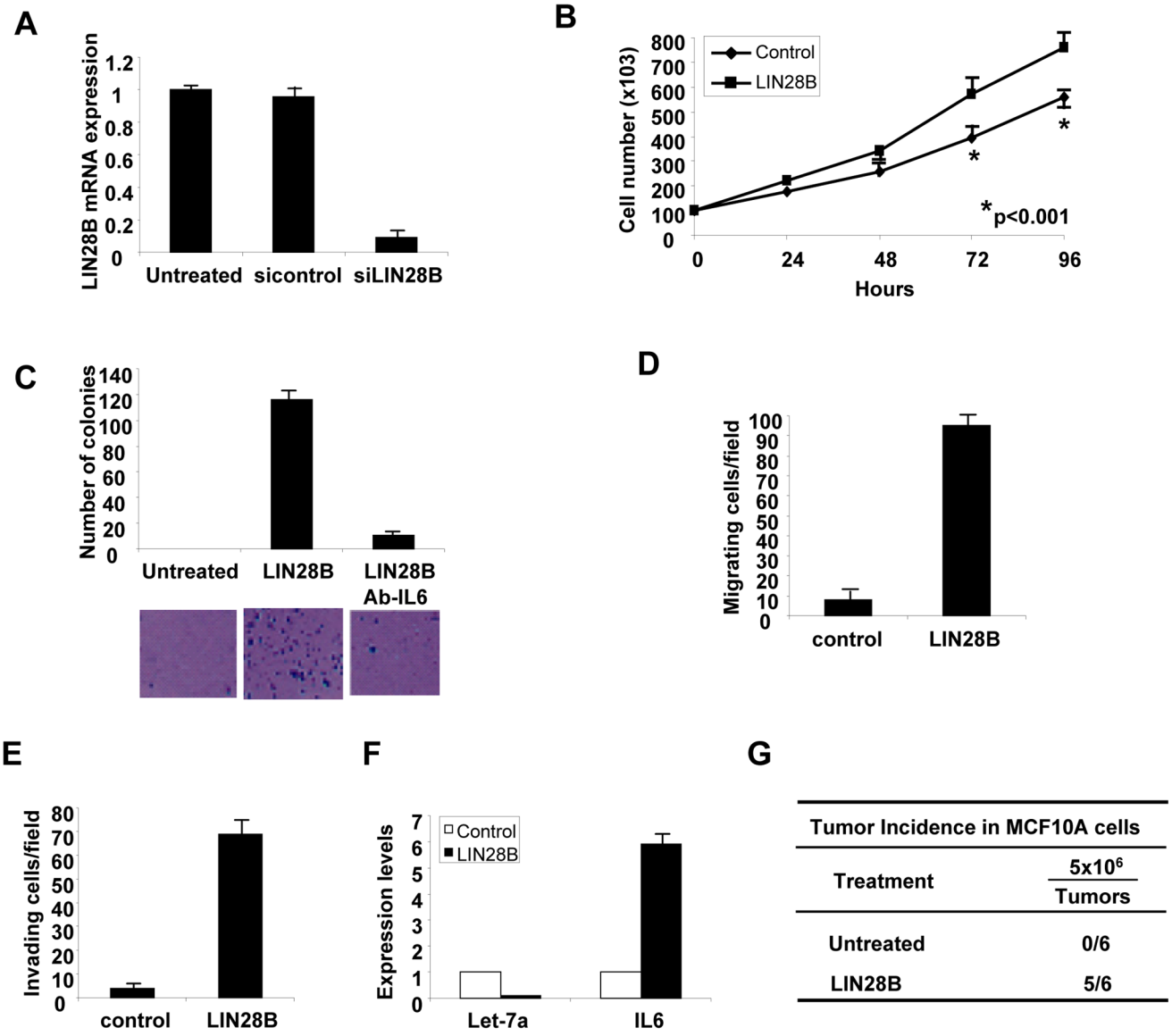

Figure S5. LIN28B overexpression promotes transformation in MCF10A cells. (A) Efficiency of LIN28B inhibition by siRNA treatment in MCF10A ER-Src cells. MCF10A ER-Src cells were treated with siRNA control and siRNA against LIN28B (80uM) and LIN28B expression was evaluated by real-time PCR, 24h post transfection. The experiment was performed in triplicate and data represent mean ± SD. **(B)** MCF10A cells were transfected with pBabe.Puro-LIN28B and cells growth was evaluated every day for 4 days. **(C)** MCF10A cells and MCF10A cells over-expressing LIN28B treated with 2ug/ml Ab-IL6 were plated in soft agar and colonies were stained with crystal violet and counted 15 days later. **(D)** Migration assay and **(E)** invasion assay of MCF10A cells and MCF10A cells transfected with pBabe.Puro-LIN28B for 48h. **(F)** Real-time PCR analysis of let-7a and IL6 mRNA expression levels in MCF10A cells transfected with pBabe.Puro-LIN28B for 48h. All the experiments described above have been performed in triplicate and represent mean ± SD. **(G)** Tumor formation in mice injected subcutaneously in their right flank with MCF10A cells and MCF10A cells transfected with pBabe.Puro-LIN28B for 48h. Tumor growth was monitored every 5 days up to 30 days by observation and palpation.

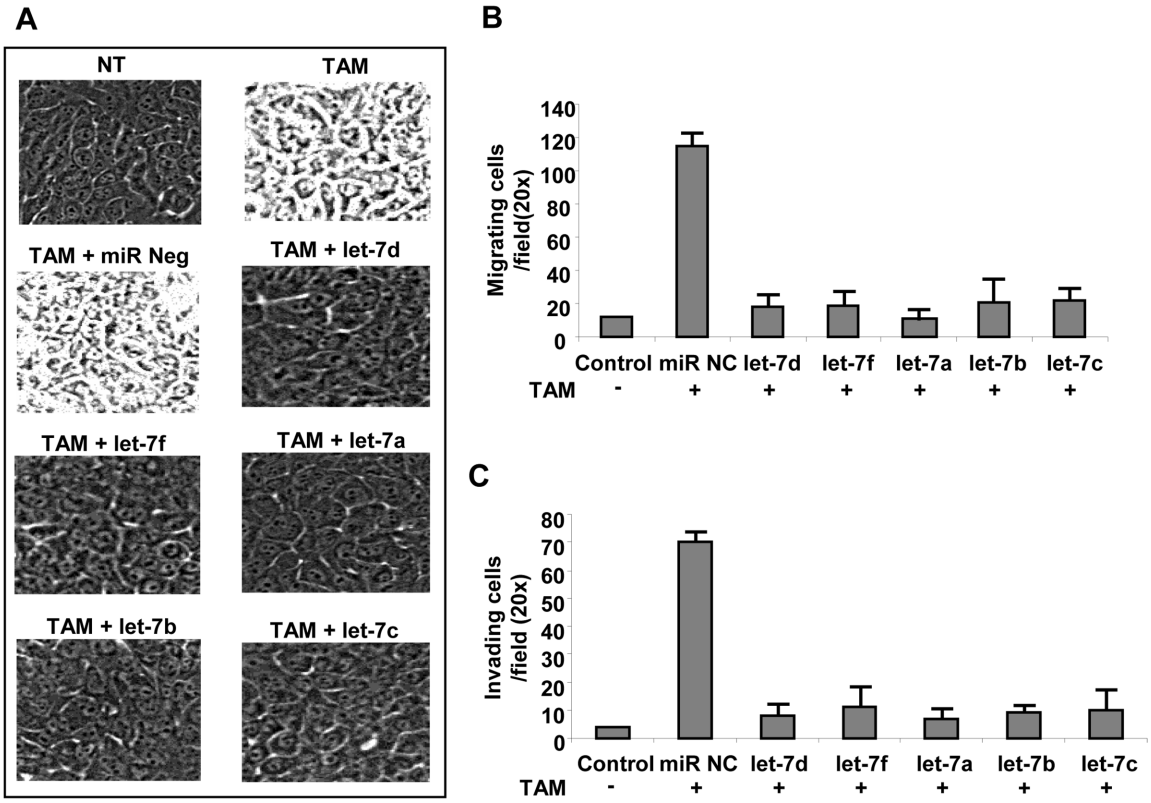

Figure S6. Inhibition of let-7 blocks MCF10A ER-Src transformation. **(A)** Phase contrast images showing the phenotypic (no formation of foci) inhibition of transformation after let-7a, let-7b, let-7c, let-7d and let-7f overexpression (100 nM) in MCF10A ER-Src TAM-treated cells. Transfection of a microRNA negative control together with 4OHT (for 36h) was used as a control. **(B)** Transwell migration assay of transformed MCF10A cells expressing let-7 family members. The columns represent the number of motile cells per field from three independent experiments. **(C)** Transwell invasion assay of transformed MCF10A cells expressing let-7 family members. The columns represent the number of motile cells per field from three independent experiments.

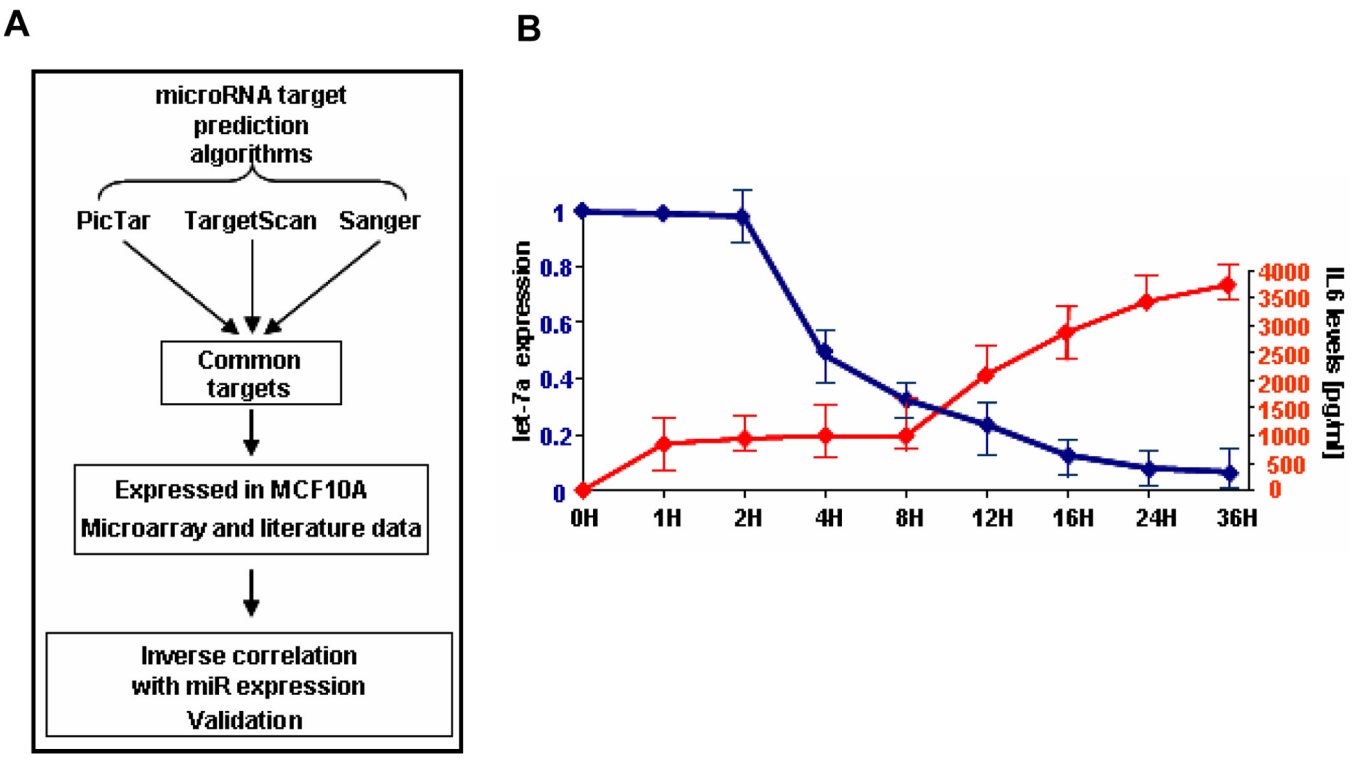

Figure S7. Integrative approach for identification of microRNA-gene targets pairs during cellular transformation. (A) The first criterion was to use identify microRNA gene targets that were common between 3 different prediction algorithms (PicTar, TargetScan, Sanger). The next criterion was to select which of these common targets are expression in MCF10A cells according to our cDNA microarray (Hirsch et al) and literature data. Finally, due to the fact that microRNAs are negative regulators of gene expression we selected only the predicted gene targets that were inversely correlated with microRNA expression. **(B)** Let-7a expression (blue color) and IL6 protein expression levels (red color) during cellular transformation assessed by real-time PCR and ELISA assays respectively. The data show the inverse correlation between let-7a and IL6 expression during MCF10A ER-Src cellular transformation.

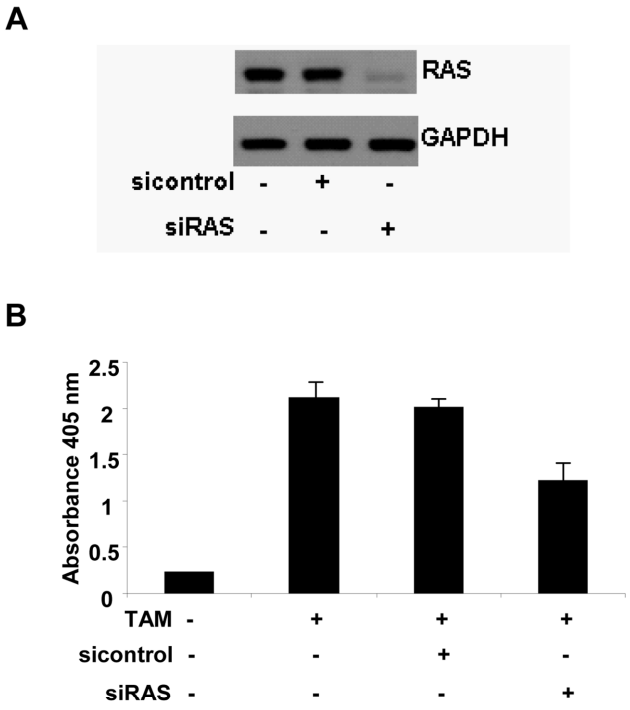

Figure S8. Antisense Ras inhibition affects partially NF-κB activity in MCF10A ER-Src TAM-treated cells. (A) RAS protein levels after treatment for 24h with siRNA control or siRNA against RAS (100nM). **(B)** Assessment of NF-KB activity in untreated and TAM-treated MCF10A ER-Src cells after treatment for 24h with siRNA against RAS (100nM).

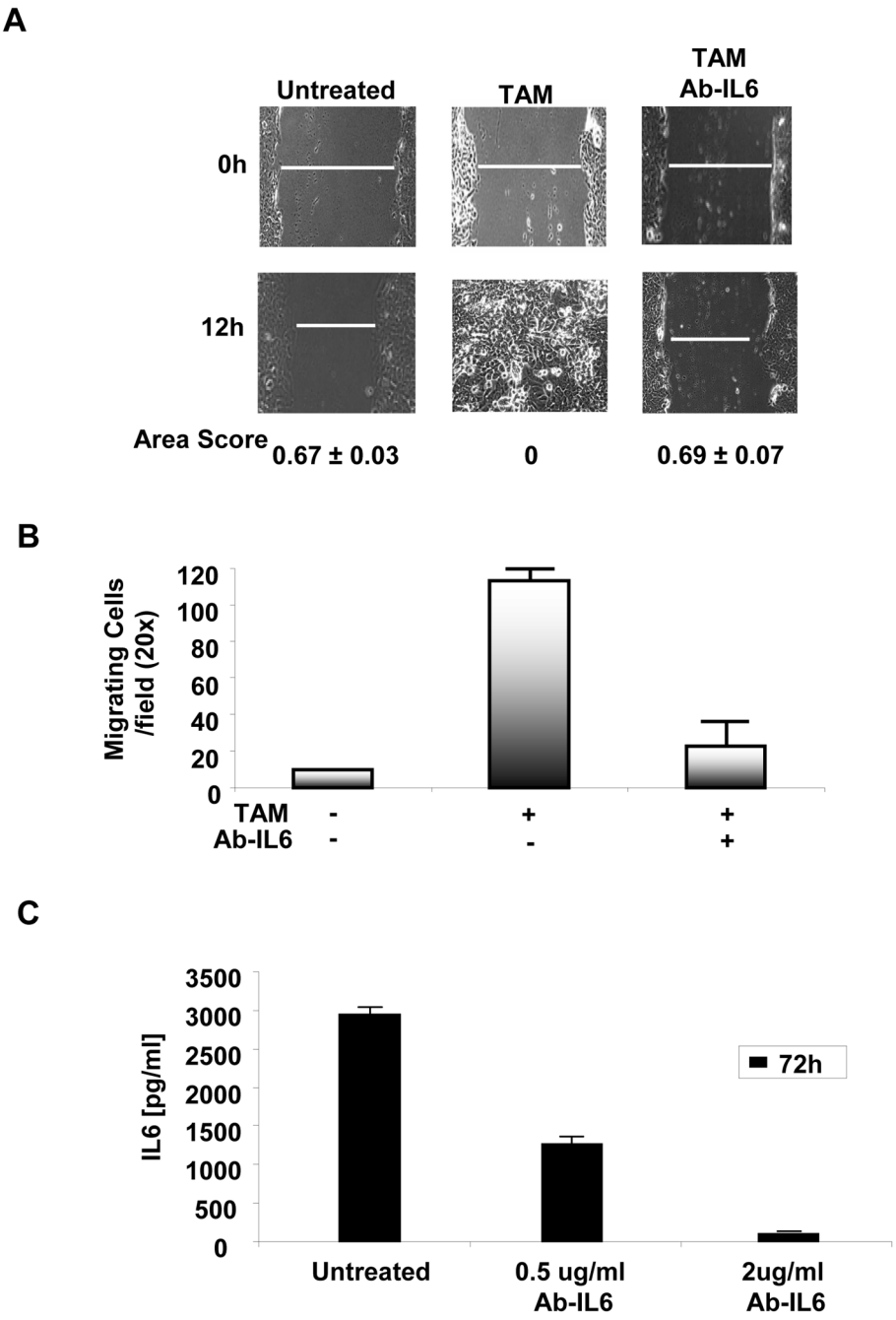

Figure S9. IL6 inhibition blocks MCF10A ER-Src cell motility. (A) Wound healing and **(B)** cell migration assays of MCF10A ER-Src cells (untreated, 1uM TAM-treated, 1uM TAM and 2 ug/ml Ab-IL6 treated). Data are represented as mean ± SD of three independent experiments. Area score was calculated using MetaMorph v5.0 program. **(C)** IL6 expression in MCF10A ER-Src cells after inhibition with IL6 monoclonal antibody. Assessment of IL6 production by ELISA assay in MCF10A ER-Src cells 72h after TAM-induction and treatment with monoclonal antibody against IL6 (2 different concentrations). The experiment has been performed in triplicate and data represent mean ± SD.

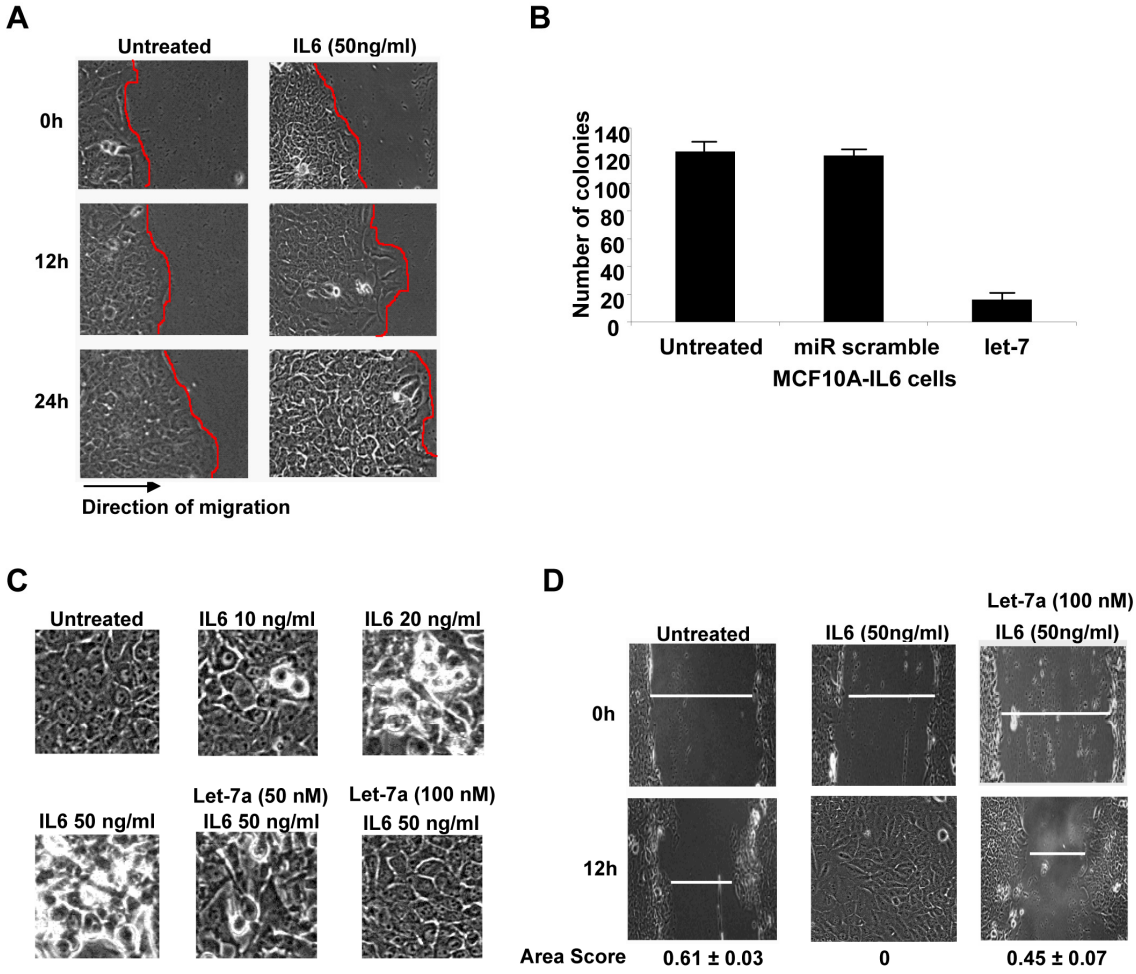

Figure S10. Motility and tumorigenicity of MCF10A IL6-transformed cells (A) IL6 affects MCF10A cell motility and morphology. Analysis of cell morphology in a wound healing experiment using MCF10A cells treated with IL6 (50ng/ml). Representative images of MCF10A cells at the wound edge. All images were taken in the same position 12 and 24h after wound healing at 20x magnification. Very interestingly IL6-treated MCF10A cells move faster closing the wound and the cells at the wound edge have a more aggressive fibroblast-like shape (look right edge of image taken from IL6 treated cells for 12h). **(B)** Overexpression of let-7 inhibits tumorigenicity of MCF10A-IL6 transformed cells. MCF10A IL6-treated cells (15 days post IL6 induction of transformation) were transfected with 100uM microRNA scramble (control) or 100uM let-7 microRNA. 24h later the cells were plated in soft agar. Colonies were stained and counted 15 days later. The experiment has been performed in triplicate and data represent mean ± SD. **(C)** MCF10A cells were treated with IL6 (10-50ng/ml) for 1h. We identified that MCF10A cells treated with 50ng/ml of IL6 for 1h transformed in 5 days. In these cells inhibition of let-7 expression inhibited the transformed phenotype. **(D)** Would healing assay in MCF10A cells treated with 50ng/ml of IL6 for 1h and then transformed in 5 days. In these cells we transfected 100nM let-7a for 24h and then performed the wound healing assay. Area score was calculated using MetaMorph v5.0 program.

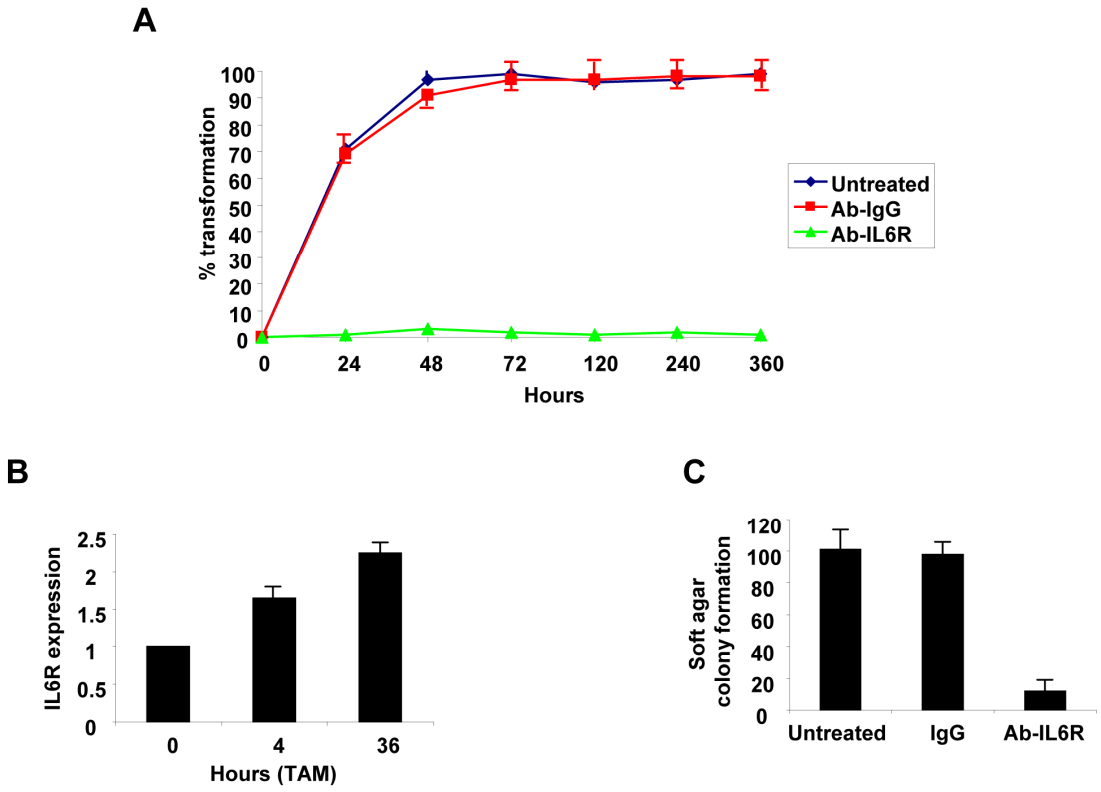

Figure S11. IL6 receptor inhibition blocks tumorigenicity of MCF10A ER-Src TAM-treated cells. (A) MCF10A ER-Src TAM-treated cells were treated with 4ug/ml of an antibody against IL6 receptor (IL6R) or isotype antibody (IgG) as a control. Inhibition of IL6 receptor blocked completely MCF10A ER-Src transformation. **(B)** IL6 receptor mRNA expression levels in untreated (0h) and 4 and 36h TAM-treated MCF10A ER-Src cells. **(C)** MCF10A ER-Src TAM-treated cells (10 days post TAM-induction) were treated with antibody against IL6 receptor for 48h and plated in soft agar. Colonies were counted 15 days later. The experiment has been performed in triplicate and data represent mean ± SD.

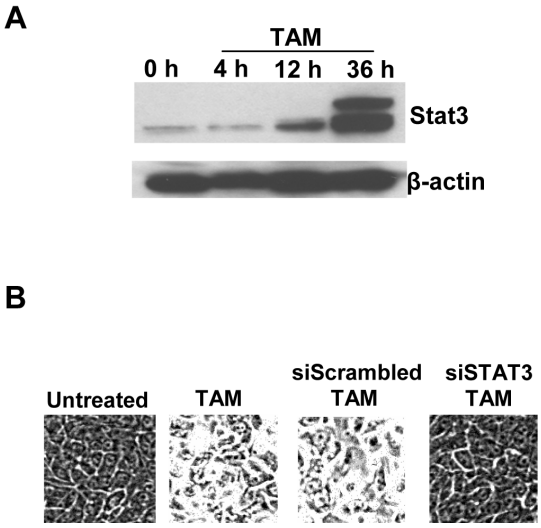

Figure S12. Stat3 inhibition affects MCF10A ER-Src transformation. (A) Stat3 protein levels during TAM-induced transformation of MCF10A ER-Src cells. B-actin levels were used as loading control. **(B)** Phase contrast images of untreated, TAM-treated, TAM-treated together with 80nM siRNA scramble and TAM-treated together with 80uM siRNA against Stat3 MCF10A ER-Src cells.

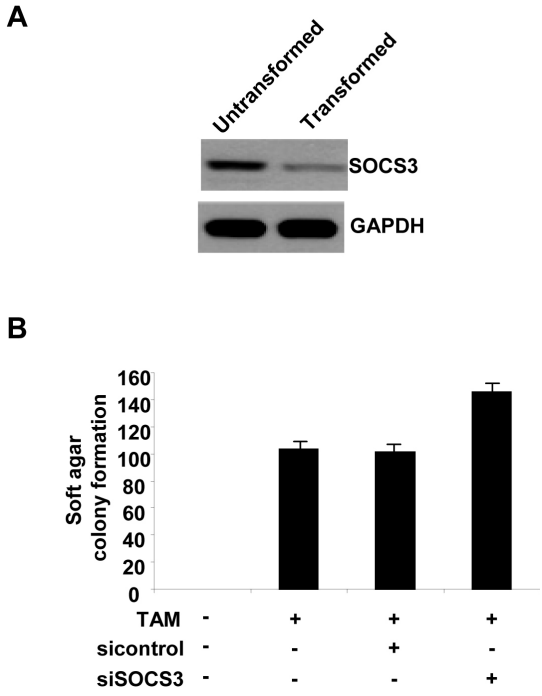

Figure S13. Socs3 inhibition increases tumorigenicity of MCF10A ER-Src TAM-treated cells. (A) Socs3 protein expression levels in untransformed MCF10A ER-Src cells and transformed (10 days post TAM-induction) MCF10A ER-Src cells. GAPDH expression levels were used as loading control. **(B)** Colony formation assay in MCF10A ER-Src cells treated with tamoxifen for 36h together with 100 nM sicontrol or 100 nM siRNA against Socs3. The experiment has been performed in triplicate and data represent mean ± SD.

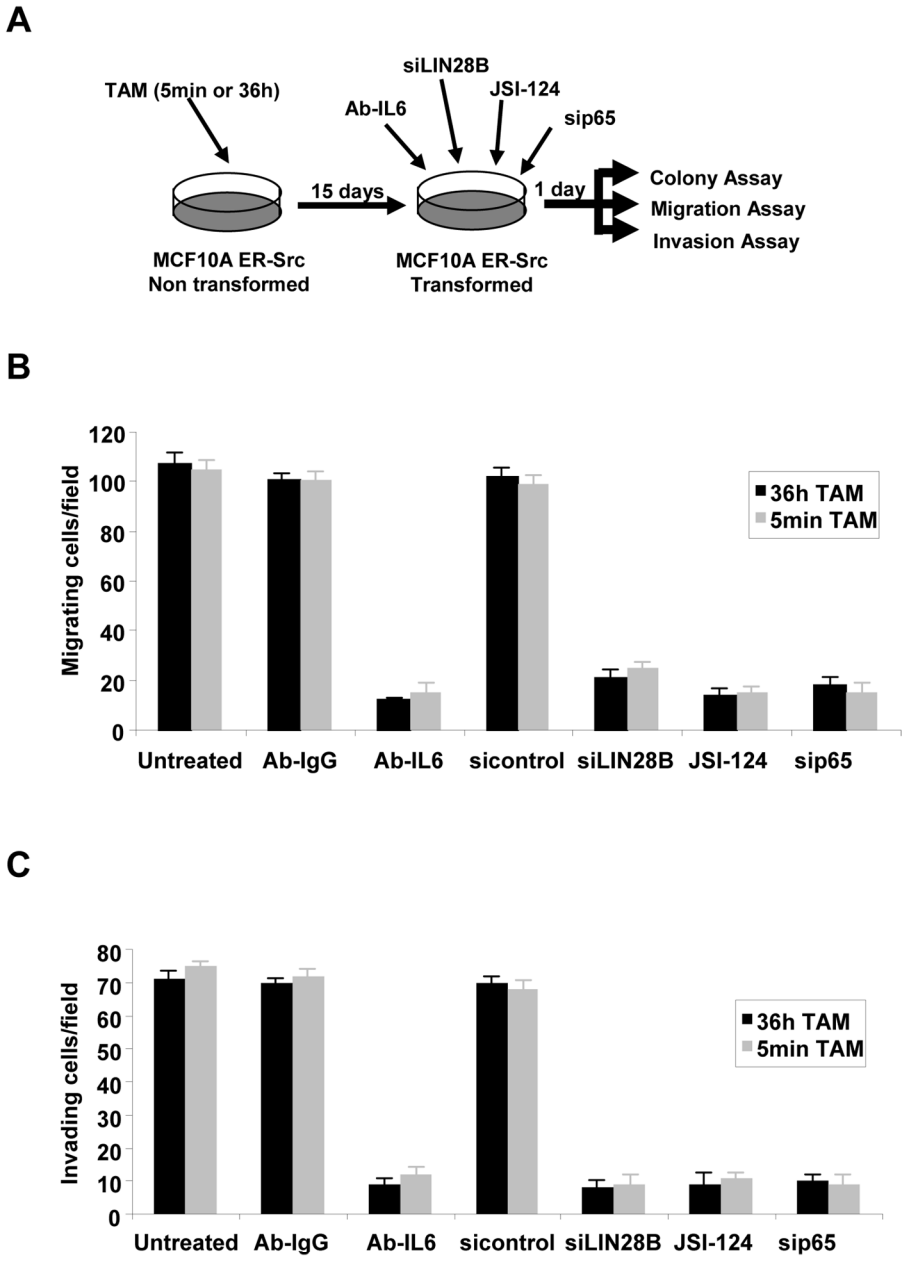

Figure S14. Perturbation of the positive feedback loop circuit blocks MCF10A ER-Src transformed phenotype. (A) Schematic of evaluating the effect of perturbating the expression of IL6 (2ug/ml monoclonal antibody against IL6), LIN28B (80uM siRNA against LIN28B), STAT3 (7uM JSI-124) and NF-KB (80uM siRNA against p65) in 5min or 36h TAM-treated MCF10A ER-Src cells. **(B)** Migration and **(C)** invasion assays of MCF10A ER-Src transformed cells 24h after different treatments. The experiment has been performed in triplicate and data represent mean ± SD.

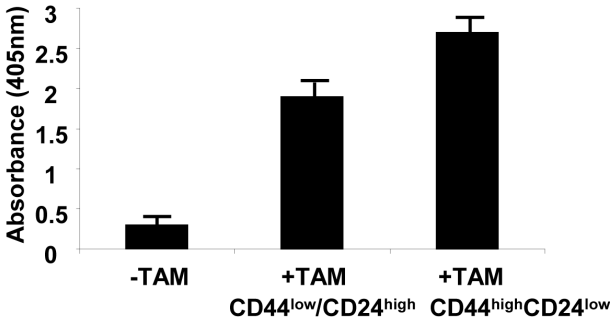

Figure S15. NF-κB activity in MCF10A ER-Src cells according to their CD44/CD24 antigen profile. NF-κB activity was assessed by ELISA assay in untreated and TAM-treated CD44low/CD24high and CD44high/CD24low MCF10A ER-Src cells. The experiment has been performed in triplicate and data represent mean ± SD.

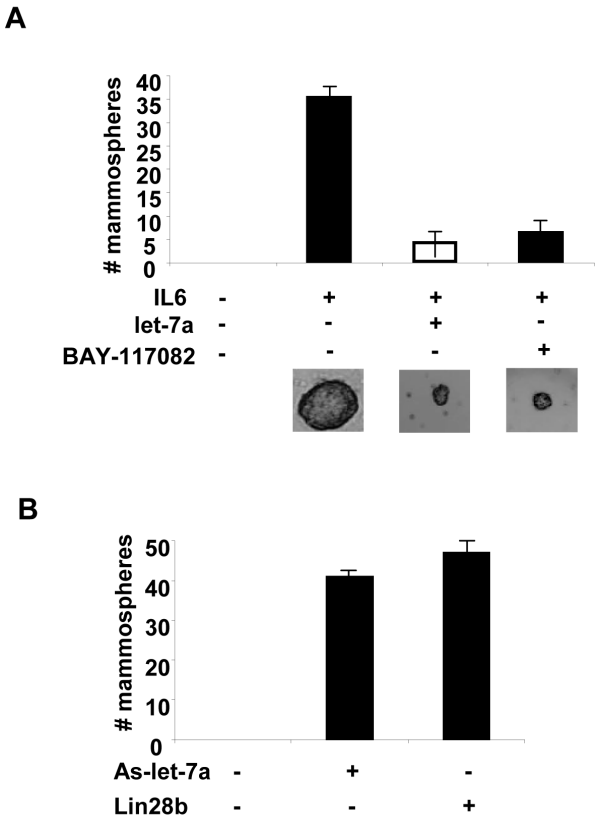

Figure S16. IL6 overexpression, let-7a inhibition and lin28b overexpression induces mammosphere formation in MCF10A cells. (A) Mammosphere formation in MCF10A cells after IL6 overexpression. Quantification and representative phase-contrast images of MCF10A mammospheres formed after IL6 (50ng/ml) and let-7a (100nM) or BAY-117082 (5 uM) treatments. The data are reported as the number of mammospheres formed/1000 seeded cells ± SD. **(B)** Mammosphere formation in MCF10A cells after inhibition of let-7a or overexpression of lin28b. MCF10A cells were transfected with 100nM as-let-7a or pBabe.Puro-LIN28B for 24h and placed on mammosphere cultures. Number of mammospheres/1000 cells were counted 7 days later. The experiment has been performed in triplicate and data represent mean ± SD.

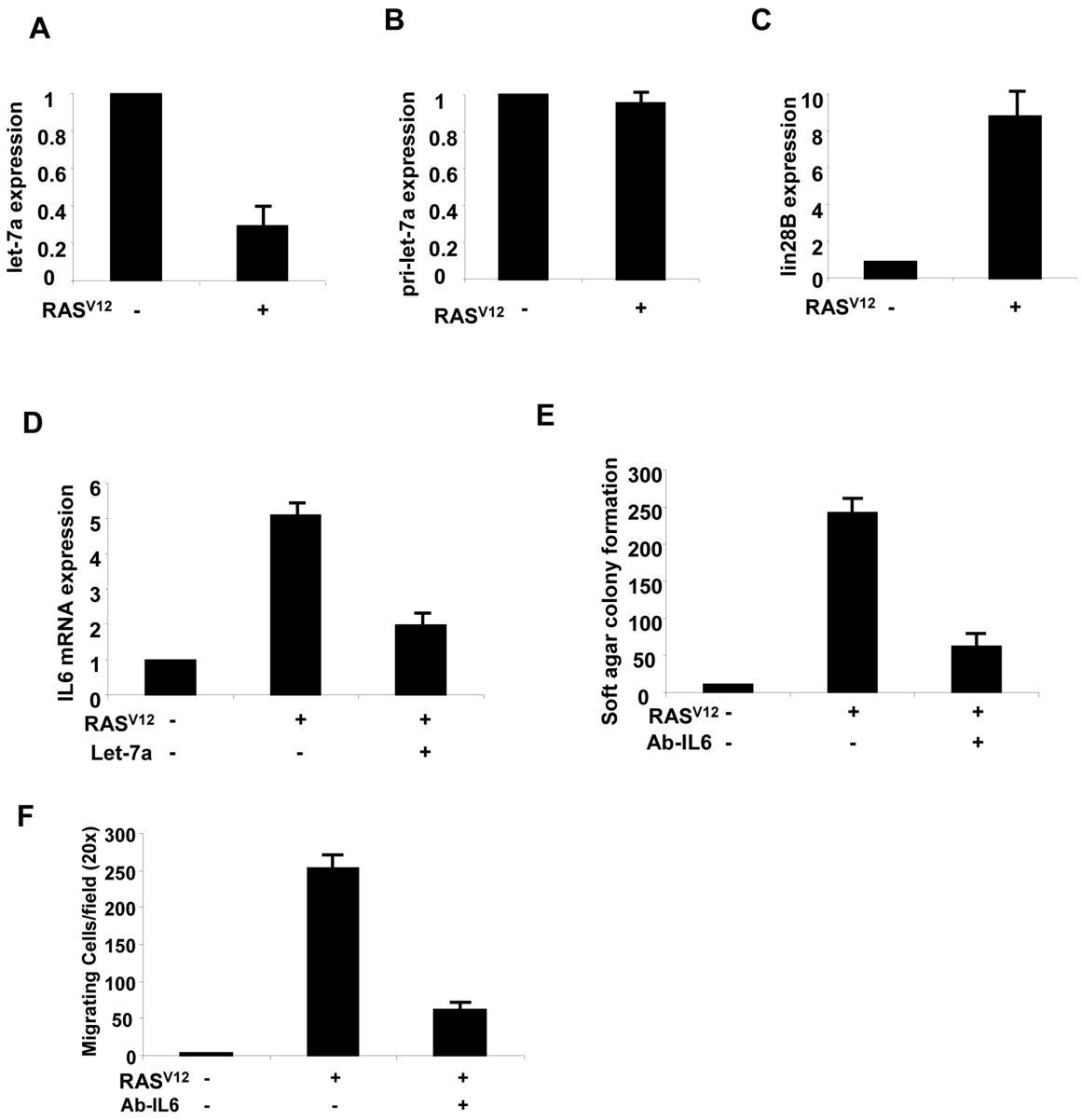

Figure S17. Lin28b, Let-7 and IL6 Circuit in MCF10A RASV12 transformation model. (A) Real-time PCR analysis of let-7a in MCF10A and MCF10A-RASV12 transfected cells (24h); **(B)** Real-time PCR analysis of pri-let-7a in MCF10A and MCF10A-RASV12 transfected cells (24h); **(C)** Real-time PCR analysis of lin28B in MCF10A and MCF10A-RASV12 transfected cells (24h); **(D)** Real-time PCR analysis of IL6 mRNA expression in MCF10A and MCF10A Ras transfected cells together with let-7a (24h); **(E)** Soft agar colony formation assay of MCF10A cells transfected with RAS for 24h and/or Ab-IL6 (2 ug/ml); **(F)** Transwell migration assay of MCF10A cells transfected with RAS for 24h and/or Ab-IL6 (2 ug/ml).

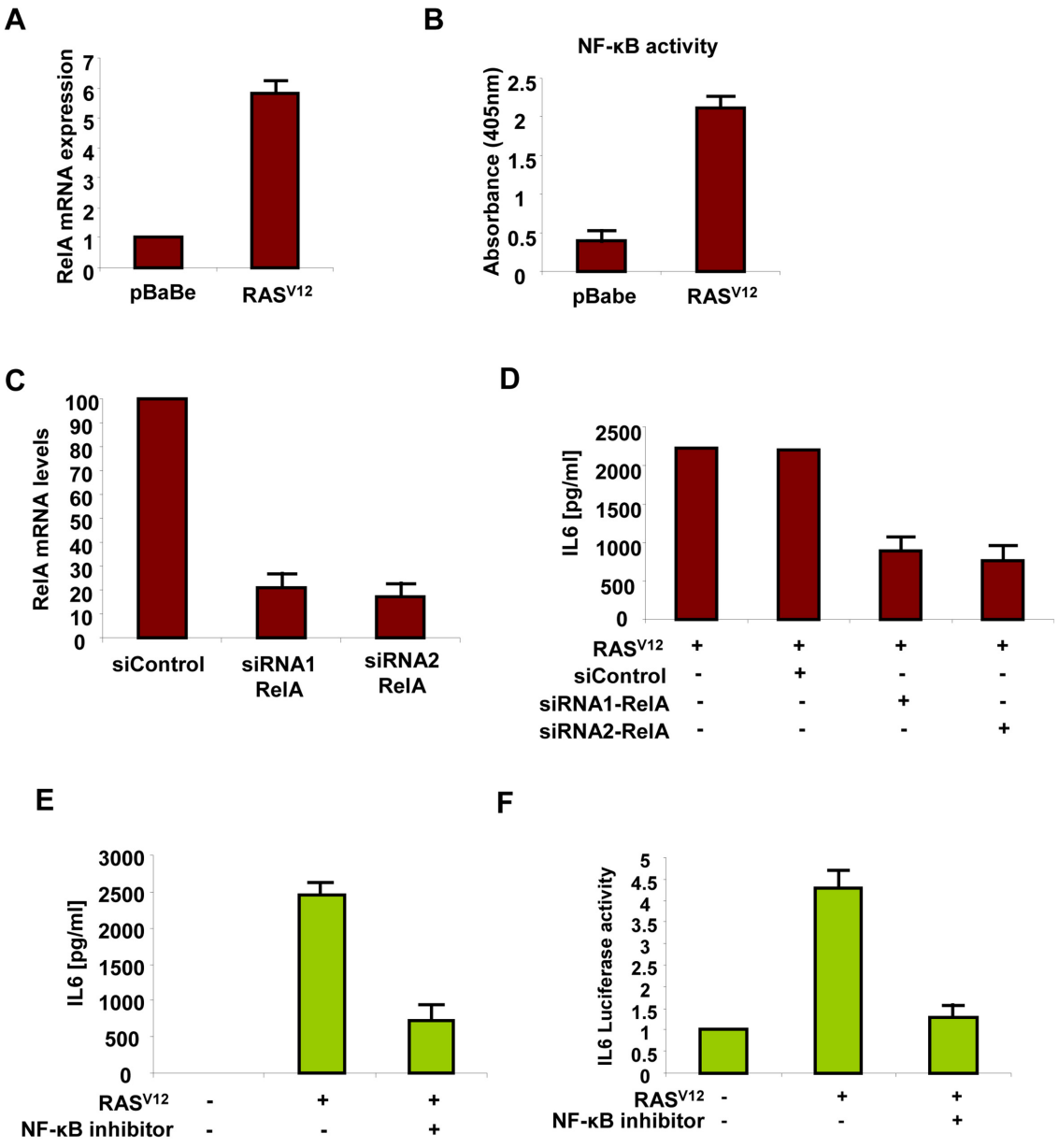

Figure S18. RASV12 affects IL6 expression through NF-kB regulation in a RASV12-induced MCF10A transformation model. (A) Real-time PCR analysis of RelA (p65) mRNA expression after RASV12 overexpression in MCF10A cells; **(B)** NF-kB/p65 ActivELISA assay (absorbance at 405nm) in RASV12-transfected MCF10A cells; **(C)** Real-time PCR analysis of RelA mRNA expression after transfection with 2 different siRNAs (80nM) against RelA; **(D)** IL6 production assessed by ELISA assay 24h after RASV12 and siRNA against RelA transfections; **(E)** IL6 production levels (ELISA assay) 24h after overexpression of RASV12 in MCF10A and/or NF-κB inhibitor (5 uM BAY-117082) treatment; **(F)** IL6 luciferase assay, 24h after overexpression of Ras in MCF10A and/or NF-κB inhibitor (5 uM BAY-117082) treatment.

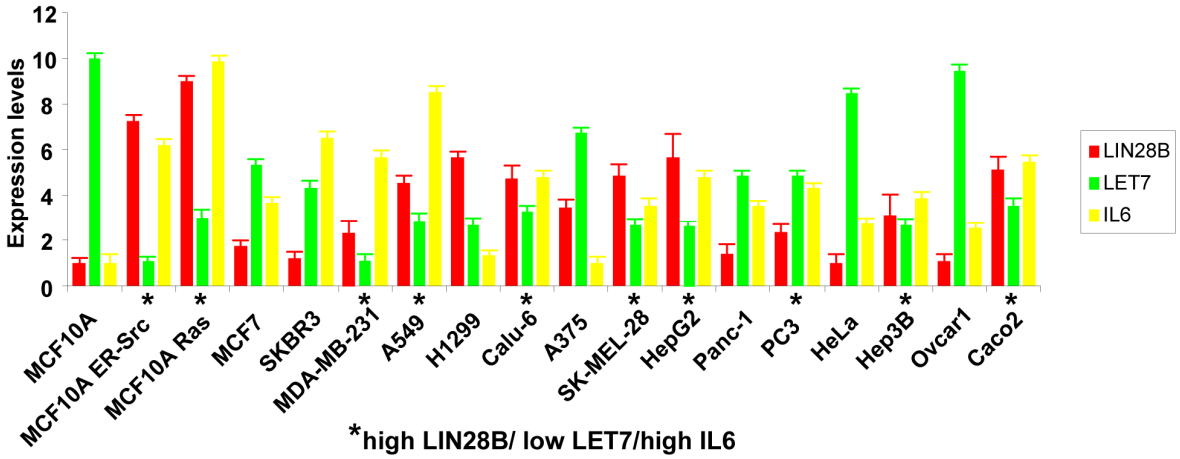

Figure S19. Lin28b, let-7 and IL6 expression levels in transformation models and cancer cell lines. Evaluation of the expression levels of lin28b, let-7 and IL6 in MCF10A cells, two transformation systems (MCF10A ER-Src, MCF10A Ras) and 3 breast (MCF7, SKBR3, MDA-MB-231), 3 lung (A549, H1299, Calu-6), 2 melanoma (A375, SK-MEL-28), 2 hepatocellular (HepG2, Hep3B), 1 pancreatic (Panc-1), 1 prostate (PC3), 1 ovarian (Ovcar1) and 1 colon (Caco2) cancer cell lines. Expression levels of lin28b, let-7 and IL6 in transformation systems and cancer cell lines were normalized to MCF10A lin28b, let-7 and IL6 expression levels. MCF10A cell line has very low levels of lin28b and IL6 while let-7 is highly expressed. The experiment was performed in triplicate and data represent mean ± SD.

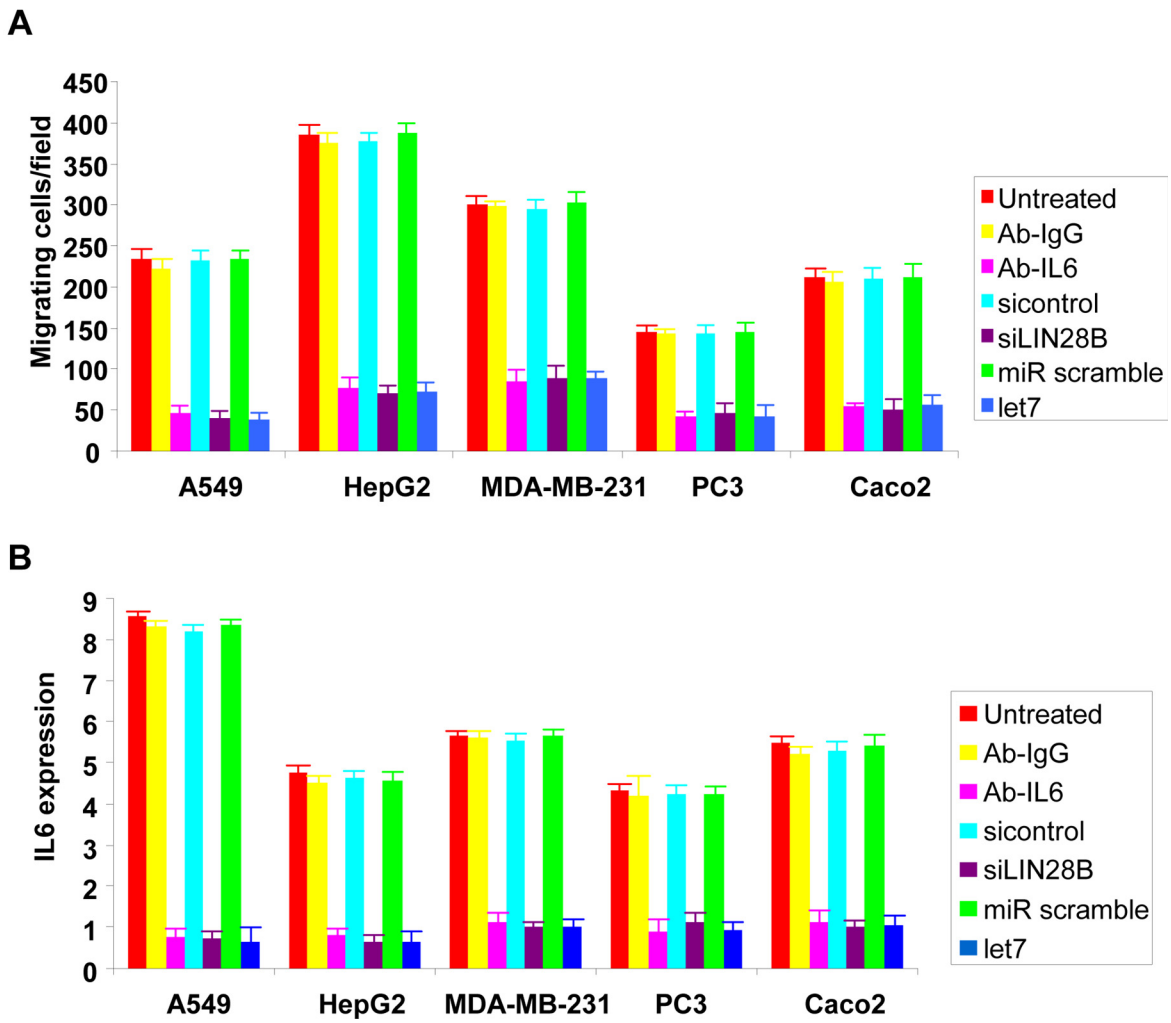

Figure S20. Perturbation of the regulatory circuit affects motility and IL6 expression in cancer cells. (A) Assessment of cell migration and **(B)** IL6 mRNA expression levels in A549, HepG2, MDA-MB-231, PC3 and Caco2 cancer cells after inhibition of IL6 (2ug/ml) expression by monoclonal antibody, inhibition of lin28b by siRNA (80nM) and overexpression of let-7 (100 nM). Treatments with IgG antibody (2ug/ml), siRNA control (80nM) and scramble miR (100 nM) were used as experimental controls. The experiment was performed in triplicate and the mean ± SD is shown.

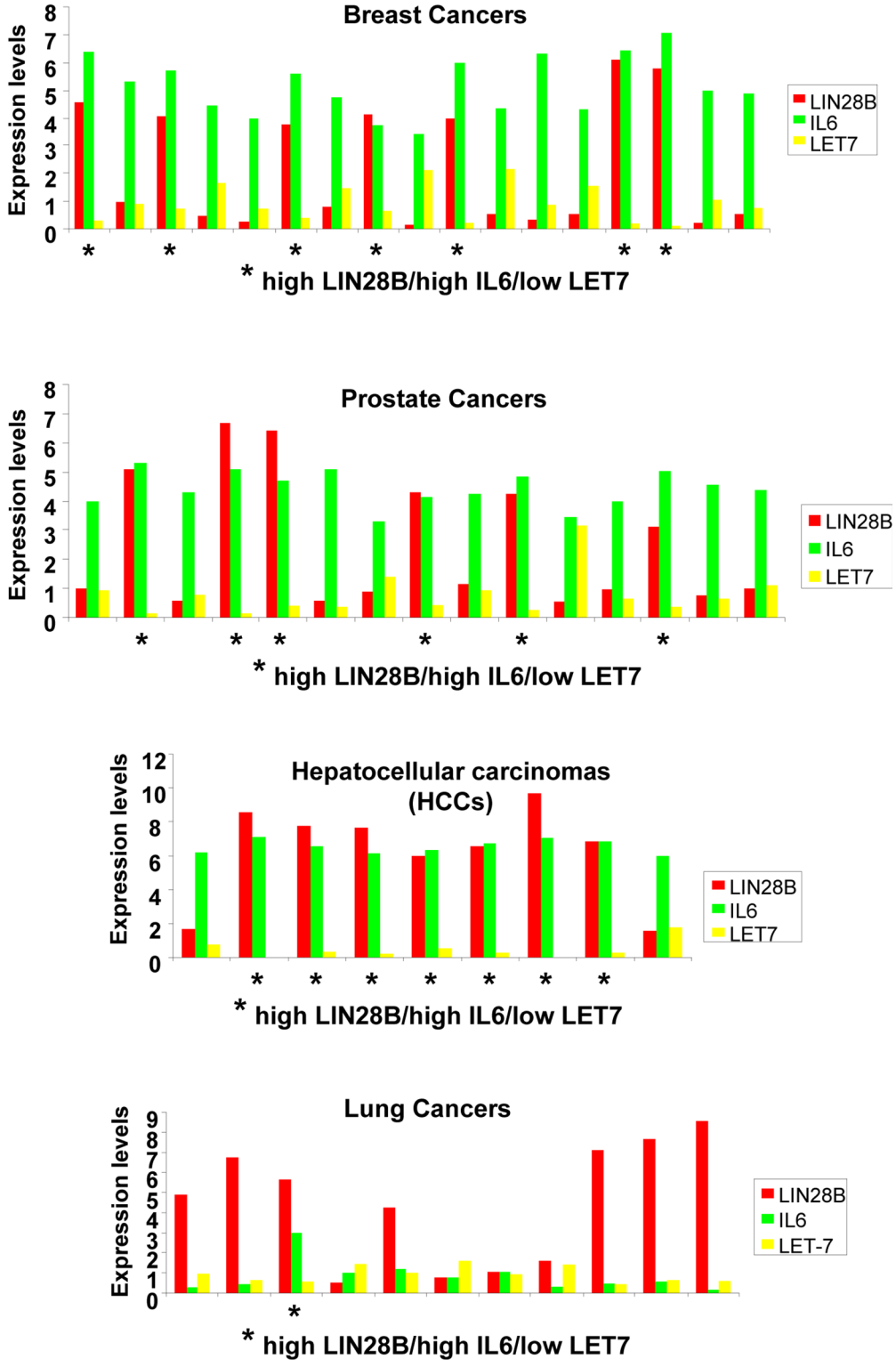

Figure S21. LIN28B, let-7 and IL6 expression levels in breast, prostate, hepatocellular and lung cancers. Identification of 7/17 breast, 6/15 prostate, 7/9 hepatocellular and 1/11 lung tumors having high LIN28B, low let-7 and high IL6 expression levels by real-time PCR analysis. Each sample was run in triplicate and the data represent the mean ± SD.

SUPPLEMENTAL REFERENCES

Chang TC, Zeitels LR, Hwang HW, Chivukula RR, Wentzel EA, Dews M, Jung J, Gao P, Dang CV, Beer MA, Thomas-Tikhonenko A, Mendell JT. (2009). Lin-28B transactivation is necessary for Myc-mediated let-7 repression and proliferation. Proc Natl Acad Sci U S A. *106*, 3384-9.

Isakoff, S.J., Engelman, J.A., Irie, H.Y., Luo, J., Brachmann, S.M., Pearline, R.V., Cantley, L.C., Brugge, J.S. (2005). Breast cancer-associated PIK3CA mutations are oncogenic in mammary epithelial cells. Cancer Res. *65*, 10992-1000.

Gunawardane, R.N., Sgroi, D.C., Wrobel, C.N., Koh, E., Daley, G.Q., Brugge, J.S. (2005). Novel role for PDEF in epithelial cell migration and invasion. Cancer Res. *65*, 11572-80.

Dontu, G., Abdallah, W.M., Foley, J.M., Jackson, K.W., Clarke, M.F., Kawamura, M.J., Wicha, M.S. (2003). In vitro propagation and transcriptional profiling of human mammary stem/progenitor cells. Genes Dev. *17*, 1253-70.

Yang, A., Zhu, Z., Kapranov, P., McKeon, F., Church, G.M., Gingeras, T.R., Struhl, K. (2006). Relationships between p63 binding, DNA sequence, transcription activity, and biological function in human cells. Mol Cell. *24*, 593-602.

Warner, J.B., Philippakis, A.A., Jaeger, S.A., He, F.S., Lin, J., Bulyk, M.L. (2008). Systematic identification of mammalian regulatory motifs' target genes and functions. Nat Methods. *5*, 347-53.